Supporting Information for

Discrimination between Human Colorectal Neoplasms with a Dual-Recognitive Two-Photon Probe

Hyo Won Lee,[a] Chang Su Lim,[a] Hosam Choi,[b] Myoung Ki Cho,[a] Choong-Kyun Noh,[c] Kiyoun Lee,[,b]*

Sung Jae Shin,[,c] and Hwan Myung Kim*[,a]*

[a] Department of Energy Systems Research and Department of Chemistry, Ajou University, Suwon 16499, Korea.

[b] Department of Chemistry, The Catholic University of Korea, Bucheon 14662, Korea.

[c] Department of Gastroenterology, Ajou University School of Medicine, Suwon 16499, Korea.

Table of Contents

Materials and General Methods. Reactions were carried out under a nitrogen atmosphere in flame-dried round-bottom flasks with a magnetic stirrer. All the chemicals were purchased from Sigma-Aldrich, and the solvents were distilled before use. Thin layer chromatography (TLC) glass pates (TLC Silica gel 60 F254, 1.05715.0001, Merck) were used to monitor the reaction process. The final products were purified using a medium-pressure liquid chromatograph (AI-580S, YAMAZEN) using normal universal or reverse phase C-18 column cartridges. NMR spectra were obtained using a 600 MHz NMR spectrometer (JNM-ECZ 600R, JEOL). High-performance liquid chromatography (HPLC) was conducted using an HPLC system (Alliance 2796, Waters), and high-resolution mass spectrometry was performed using a HR-MS system (Accela UPLC/LTQ-Orbitrap XL, Thermo Fisher Scientific) from Gyeonggido Business & Science Accelerator (GBSA, Korea).

Synthetic Route for **GS** and **SGG**. Compounds **1**, **2**, and **4** were prepared by following the literature methods,[1–3] and synthetic procedures of other compounds are described below.

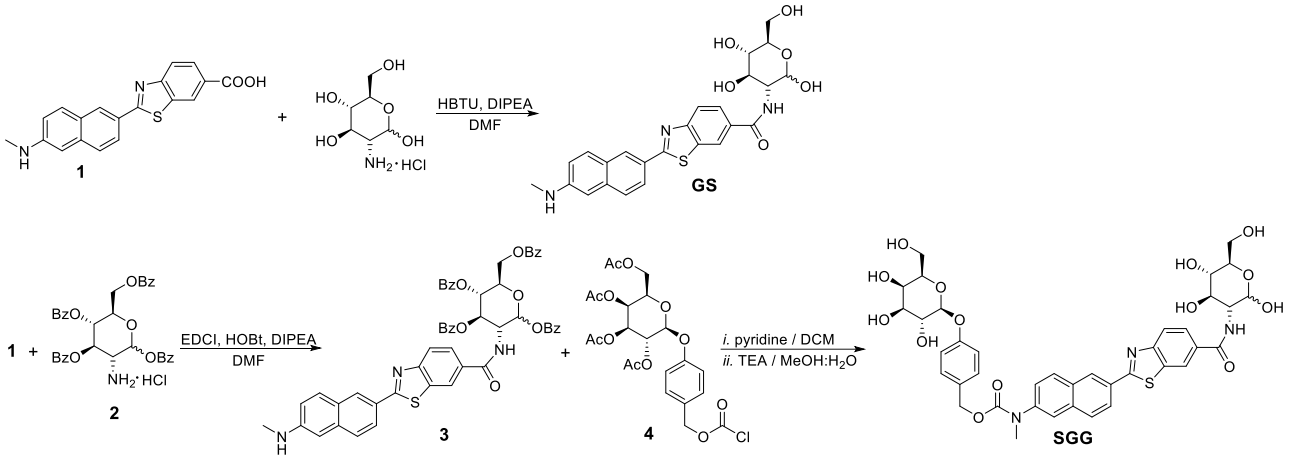

Scheme S1. Synthesis of **GS** and **SGG**.

Synthesis of **GS**. A solution of **1** (14.8 mg, 0.044 mmol, 1.0 eq.) and *N*,*N*,*N*′,*N*′-tetramethyl-*O*-(1*H*-benzotriazol-1-yl)uronium hexafluorophosphate (HBTU, 25.2 mg, 0.066 mmol, 1.5 eq.) in DMF (0.4 mL) was treated with DIPEA (15 μL, 0.09 mmol, 2 eq.) and the reaction mixture was stirred for 1 h at 25 °C before it was treated with D-(+)-glucosamine hydrochloride (10.4 mg, 0.048 mmol, 1.1 eq.). After stirring for additional 3 h at 25 °C, the resulting mixture was quenched with saturated aqueous $NaHCO_3$ and diluted with EtOAc. The layers were separated, and the aqueous layer was extracted with a premixed solution ($CHCl_3$:*i*-PrOH = 3:1). The combined organic layers were washed with brine, dried over anhydrous Na_2SO_4, and concentrated under reduced pressure. The crude residue was purified by column chromatography (10 to 20% MeOH in DCM) to afford **GS** (25.3 mg, 71%) as yellow semi-solid. ^{1}H NMR (DMSO-d_6, 600 MHz): δ (ppm) 8.68 (s, 1H), 8.44 (s, 1H), 8.20 (d, J =

6.9 Hz, 1H), 8.05–8.01 (m, 3H), 7.83 (d, J = 9.6 Hz, 1H), 7.73 (d, J = 9.6 Hz, 1H), 7.04 (d, J = 6.9 Hz, 1H), 6.73 (s, 1H), 6.48 (d, J = 4.1 Hz, 1H), 6.43 (t, J = 4.8 Hz, 1H), 5.12 (d, J = 4.1 Hz, 1H), 4.97 (d, J = 3.4 Hz, 1H), 4.75 (d, J = 5.5 Hz, 1H), 4.45 (d, J = 5.5 Hz, 1H), 3.86–3.76 (m, 2H), 3.66 (m, 2H), 3.55–3.42 (m, 1H), 3.23–3.20 (m, 1H), 2.82 (d, J = 4.1 Hz, 3H); HRMS (ESI^+): m/z calculated for $[C_{25}H_{26}O_6N_3S]^+$: 496.1537, found: 496.1545.

Synthesis of **3**. A solution of **1** (432 mg, 1.29 mmol, 1.0 eq.), *N*-(3-dimethylaminopropyl)-*N*′-ethylcarbodiimide hydrochloride (EDCI, 297 mg, 1.55 mmol, 1.2 eq.) and 1-hydroxybenzotriazole hydrate (HOBt, 209 mg, 1.55 mmol, 1.2 eq.) in DMF (6.4 mL) was treated with DIPEA (1.12 mL, 6.47 mmol, 5.0 eq.), and stirred for 30 min at 25 °C. To this reaction mixture, **2** (981 mg, 1.55 mmol, 1.2 eq.) was added, and stirred for additional 17 h at 25 °C, the resulting mixture was quenched with saturated aqueous $NaHCO_3$, diluted and extracted with EtOAc. The combined organic layers were washed with brine, dried over anhydrous Na_2SO_4, and concentrated under reduced pressure. The residue was purified by column chromatography (2% MeOH in DCM) to provide **3** (948 mg, 80%) as green semi-solid. ^1H NMR ($CDCl_3$, 600 MHz): δ (ppm) 8.29 (s, 1H), 8.14–8.12 (m, 3H), 8.06–8.05 (m, 2H), 7.97–7.92 (m, 5H), 7.81 (d, J = 8.2 Hz, 1H), 7.67–7.63 (m, 2H), 7.59–7.53 (m, 3H), 7.50–7.40 (m, 7H), 7.36–7.30 (m, 4H), 6.88 (d, J = 8.2 Hz, 1H), 6.78–6.75 (m, 2H), 6.29 (d, J = 8.2 Hz, 1H), 5.96–5.87 (m, 2H), 5.13 (d, J = 9.6 Hz, 1H), 4.67 (dd, J = 12.3, 2.7 Hz, 1H), 4.54 (q, J = 5.5 Hz, 1H), 4.38 (t, J = 4.8 Hz, 1H), 2.96 (s, 3H) ; HRMS (ESI^+): m/z calculated for $[C_{53}H_{42}O_{10}N_3S]^+$: 912.2585, found: 912.2562.

Synthesis of **SGG**. (*i*) A cooled (0 °C) solution of **3** (740 mg, 0.811 mmol, 1.0 eq.) in DCM (4.1 mL) was treated with pyridine (0.2 mL, 2.44 mmol, 3.0 eq.). After stirring for 30 min at the same temperature, chloroformate **4** (637 mg, 1.23 mmol, 1.5 eq.) in DCM (25 mL) was added. After stirring for 1 h at 0 °C, the resulting mixture was quenched with saturated aqueous $NaHCO_3$, diluted and extracted with DCM. The combined organic layers were washed with brine, dried over anhydrous Na_2SO_4, and concentrated under reduced pressure. The residue was purified by column chromatography (2 to 3% MeOH in DCM) to afford the intermediate (719 mg, 64%) as yellow semi-solid. (*ii*) To the solution of the intermediate (121 mg, 0.094 mmol, 1.0 eq.) in MeOH:H_2O (5:1), TEA was added, and stirred for 8.5 h at 100 °C. The resulting mixture was cooled to RT and concentrated under reduced pressure. The residue was purified by a preparative C18 column (2 × 25 cm, 25 % distilled water/0.1% TFA in MeOH) to provide **SGG** TFA salt (40.1 mg) as yellow solid. To a stirred solution of **SGG** TFA salt (40.1 mg) in MeOH (30 mL), a basic resin (Amberlite® IRA-67 free base, 200 mg, 500 wt% of **SGG** TFA salt) was added and the resulting mixture was stirred for 30 min at 25 °C. The resulting mixture was filtered through a pad of celite and concentrated in vacuo to afford **SGG** (23.7 mg, 34%) as white semi-solid. ^1H NMR (DMSO-d_6, 600 MHz): δ (ppm) 8.82 (s, 1H),

8.73 (s, 1H), 8.24 (d, J = 8.3 Hz, 1H), 8.17–8.14 (m, 3H), 8.11 (d, J = 9.0 Hz, 1H), 8.06 (d, J = 9.0 Hz, 1H), 7.94 (s, 1H), 7.64 (d, J = 9.0 Hz, 1H), 7.31 (d, J = 8.0 Hz, 2H), 7.01 (d, J = 8.0 Hz, 2H), 5.13 (m, 2H), 5.10 (s, 2H), 4.99 (d, J = 7.6 Hz, 1H), 4.82 (m, 3H), 4.63 (d, J = 5.2 Hz, 1H), 4.48 (d, J = 4.8 Hz, 1H), 3.69 (m, 2H), 3.57-3.47 (m, 10H), 3.38 (s, 3H), 3.08 (m, 2H); HRMS (ESI^+): m/z calculated for $[C_{39}H_{42}O_{14}N_3S]^+$: 808.2382, found: 808.2408.

Spectroscopic Experiments. One-photon fluorescence emission experiments were conducted using a FluoroMate FS-2 (SCINCO, Korea) spectrophotometer with a temperature controller (-10–80 °C). One-photon absorption experiments were conducted using a S-3100 (SCINCO, Korea) UV-Vis spectrophotometer. The spectroscopic experiments were performed by placing the sample solutions in a 1.0 cm quartz cuvette (HE.111.650QG, Hellma Analytics). For the selectivity test, enzyme kinetics assay, and pH dependency test, a multi-detection microplate reader (Varioskan Flash, Thermo Fisher Scientific), and a 96-well microplate for fluorescence (164588, Thermo Fisher Scientific) were used. The relative quantum yield (Φ) was determined using 9,10-diphenylanthracene (Φ = 0.93 in cyclohexane), as described in literature.[4]

Water Solubility. DMSO stock solutions (10 mM) of **SGG** and **GS** were prepared and were diluted to 0.05–10.0 μM and added to a 1.0 cm quartz cuvette (HE.111.650QG, Hellma Analytics) containing 2.0 mL of PBS buffer (10 mM, pH 7.4) using a micro syringe. In all the samples, the final concentration of DMSO in the buffer was maintained as 0.1%.[5] In the fluorescence intensity versus concentration plot of each compound, the maximum concentration in the linear region was selected as the water solubility. The linear fitting was performed by using a linear function (OriginPro 8.0, OriginLab). The water solubilities of **SGG** and **GS** in buffer were approximately 5.0 μM and 3.0 μM, respectively.

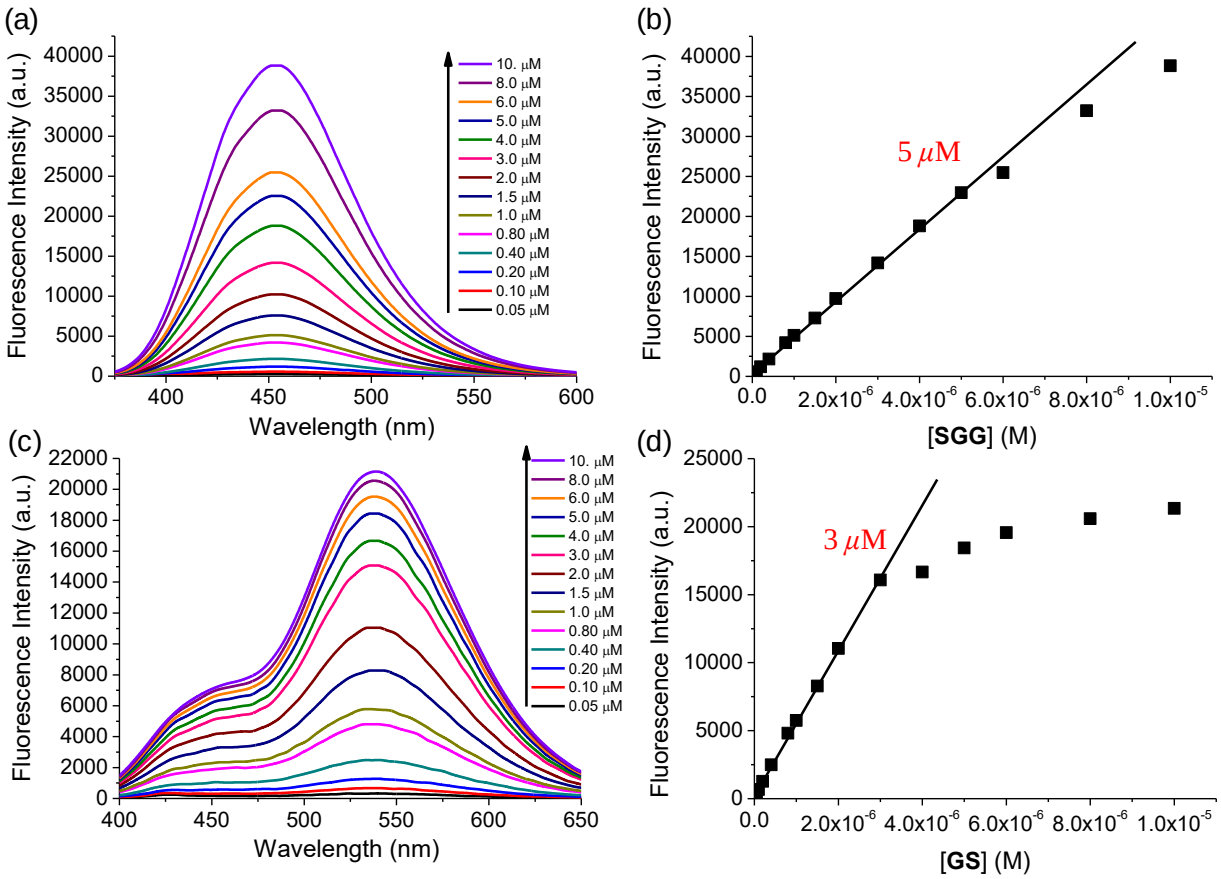

Figure S1. (a,c) One-Photon fluorescence spectra of **SGG** (a) and **GS** (c) in buffer (10 mM PBS, pH 7.4). and (b,d) plot of the fluorescence intensity against the concentration of **SGG** (b) and **GS** (d). The excitation wavelengths were 332 nm for **SGG** and 373 nm for **GS**.

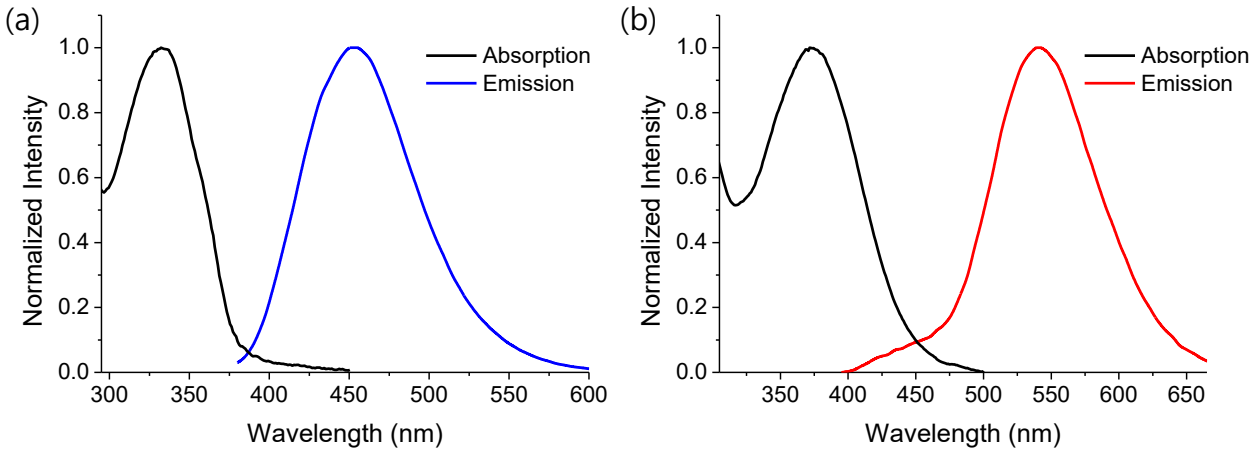

Figure S2. Normalized one-photon absorption and emission spectra of (a) **SGG** and (b) **GS** in buffer (10 mM PBS, pH 7.4).

Two-Photon Cross Section. The two-photon absorption cross section (δ) was determined by the following general method.[6] **SGG** and **GS** (1.0 μM) were dissolved in buffer (10 mM PBS, pH 7.4) and the two-photon excited emission was integrated using Rhodamine 6G as the reference compound, whose TP characterization is well established.[7] The TPEF intensities of each sample and Rhodamine 6G were detected at the same excitation wavelength (720 to 880 nm). The TP cross section was determined using $\delta = \delta_r(S_s\Phi_r\phi_r c_r)/(S_r\Phi_s\phi_s c_s)$, where the subscripts r and s indicate the reference and samples, respectively; δ_r is the TP cross section of Rhodamine 6G; S is the TPEF signals collected using a CCD system (Monora 320i monochromator with DV401A-BV detector, DONGWOO OPTRON, Korea); Φ is the fluorescence quantum yield; ϕ is the overall fluorescence collection efficiency of the experimental system, and c is the concentration of each sample.

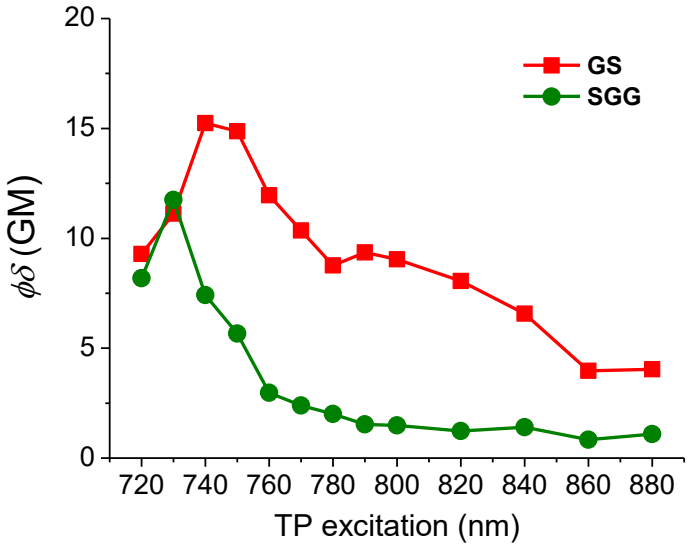

Figure S3. Two-photon action cross section of **SGG** and **GS** in buffer (10 mM PBS, pH 7.4). The estimated uncertainties for the two-photon action cross section values ($\Phi\delta$) are ± 15%.

Table S1. Photophysical properties of **SGG** and **GS** in buffer.[a]

Compound	λ^1_{max} (10^{-4} ε)[b]	λ^{fl}_{max}[c]	Φ[d]	R_{max}/R_{min}[e]	λ^2_{max}[f]	$\Phi\delta_{max}$[g]	δ_{max}[h]
SGG	332 (2.10)	453	1.00	45	730	12	12
GS	373 (1.87)	540	0.10		740	15	150

a) Measurements were performed in buffer (10 mM PBS, pH 7.4). b) λ_{max} of the absorption spectra in nm. The numbers in parentheses are molar extinction coefficients in $M^{-1}cm^{-1}$. c) λ_{max} of one-photon emission spectra in nm. d) Fluorescence quantum yields, ± 10%. e) Emission ratio (F_{green}/F_{blue}) conversion factor, R_{max}/R_{min}, measured by one-photon processes before and 30 min after the addition of 1.0 unit/mL β-galactosidase. f) λ_{max} of the two-photon excitation spectra in nm. g,h) The peak two-photon action (g) and absorption (h) cross sections in GM (1 GM = 10^{-50} cm^4 s $photon^{-1}$), ± 15%.

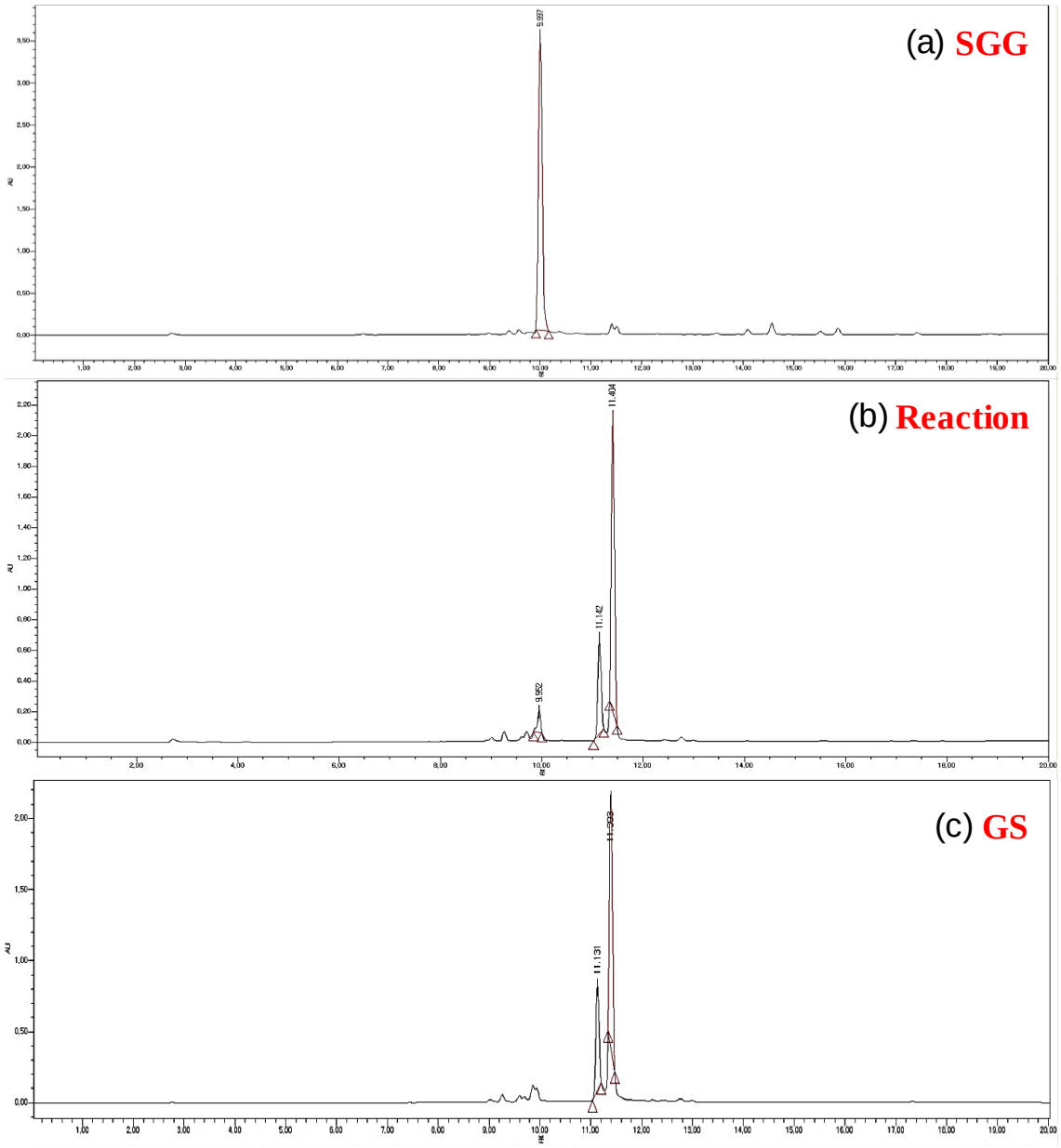

Figure S4. Confirmation of the conversion of **SGG** by β-galactosidase to **GS**. HPLC analysis of (a) **SGG**, (b) **SGG** and enzyme reaction mixture, and (c) **GS**. HPLC condition: 1.0 mL/min flow rate, 5% to 100% acetonitrile in 0.1 M triethylamine aqueous solution over 20 min. Absorbance at 370 nm was detected. Peak at 9.9 min is correspond to **SGG**, peaks at 11.1 and 11.4 min are correspond to α and β anomers of **GS**.

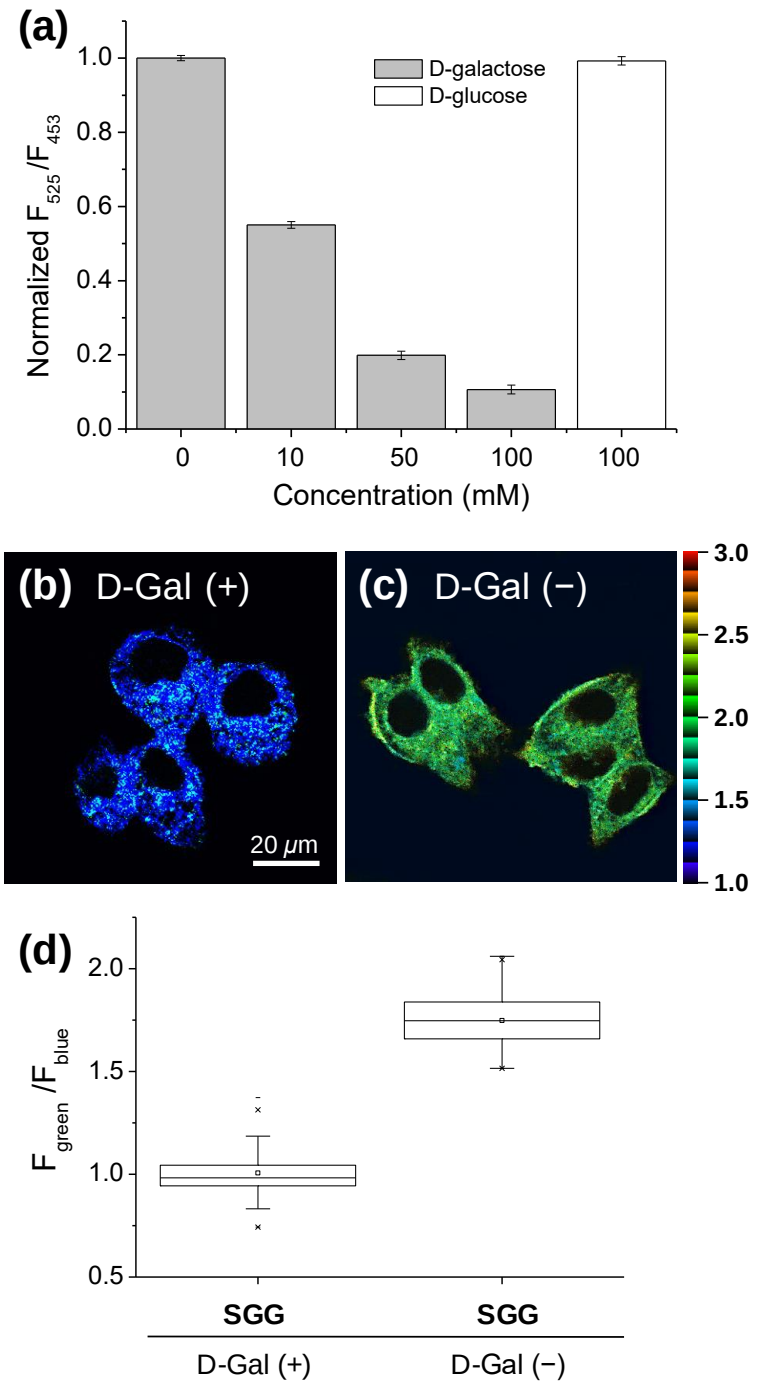

Figure S5. (a) Normalized OP fluorescence ratios (F_{525}/F_{453}) of **SGG** (1 μM) at 30 min after treatment of β-galactosidase (1 unit/mL) in buffer (10 mM PBS, pH 7.4, 37 °C) pre-treated with D-galactose (0 to 100 mM, gray bars), and D-glucose (100 mM, white bar). The excitation wavelength was 363 nm (n = 10). (b,c) Pseudocolored ratiometric TPM images (F_{green}/F_{blue}) of **SGG**-labeled HCT 116 cells pretreated with (b) or without (c) D-galactose (D-Gal, 100 mM). (d) Plot of F_{green}/F_{blue} ratios in (b) and (c). (n = 100).

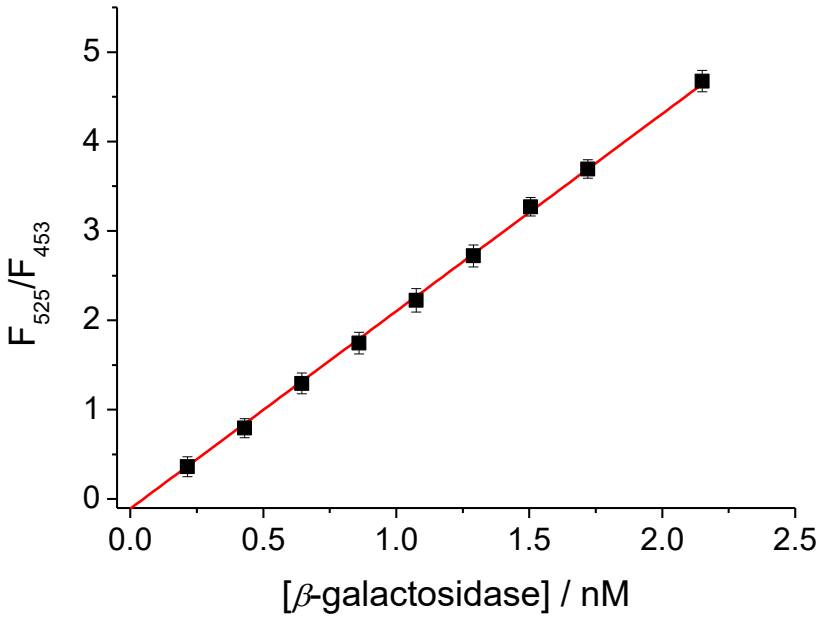

Figure S6. Plot of fluorescence ratios (F_{525}/F_{453}) for **SGG** versus [β-galactosidase]. Each data was acquired at 30 min after treatment of the enzyme in buffer (10 mM PBS, pH 7.4, 37 °C) with the excitation wavelength of 363 nm (n = 5). The detection limit value (0.04 nM) was calculated as 3σ/k; where σ is the standard deviation of ratio values in control experiments, and k is the slope of the above linear plot (red).

Enzyme Kinetics. Enzyme kinetics assays were performed using a multi-detection microplate reader. Various concentrations (0 to 40 μM) of **SGG** solution were prepared in buffer (10 mM PBS, pH 7.4, 37 °C). β-gal with a final concentration of 2.0 mg/L was used, and the fluorescence intensity was recorded at 525 nm at 1 min intervals from 0 to 60 min. The change in intensity was converted to velocity and plotted with non-linear fitting by a hyperbolic function (OriginPro 8.0, OriginLab), and the parameters of Michaelis-Menten kinetics were obtained.

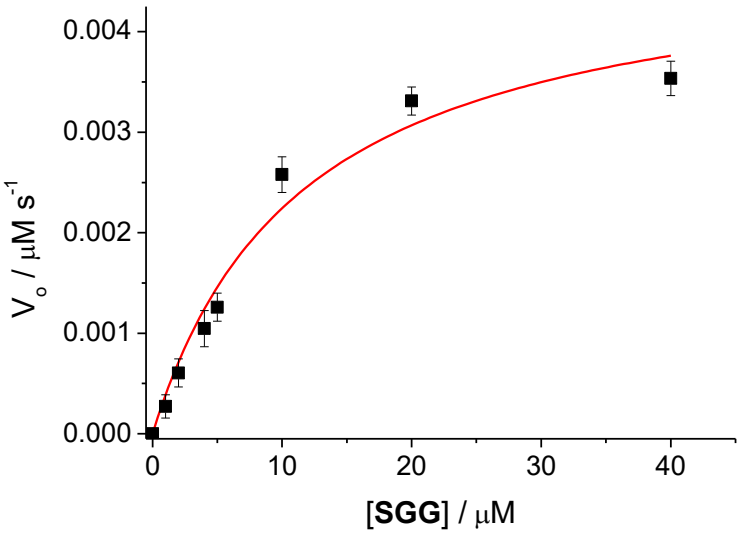

Figure S7. Michaelis-Menten plot for β-galactosidase (2.0 mg/L) with various concentrations of **SGG** in buffer (10 mM PBS, pH 7.4, 37 °C) (n = 5).

Table S2. Kinetic parameters for **SGG** with β-galactosidase.

Compound	K_m (μM)	k_{cat} (s^{-1})	k_{cat}/K_m ($\mu M^{-1}\ s^{-1}$)	V_{max} (nmol $mg^{-1}\ s^{-1}$)
SGG	11.65 ± 2.65	1.13 ± 0.11	0.097 ± 0.031	2.43 ± 0.23

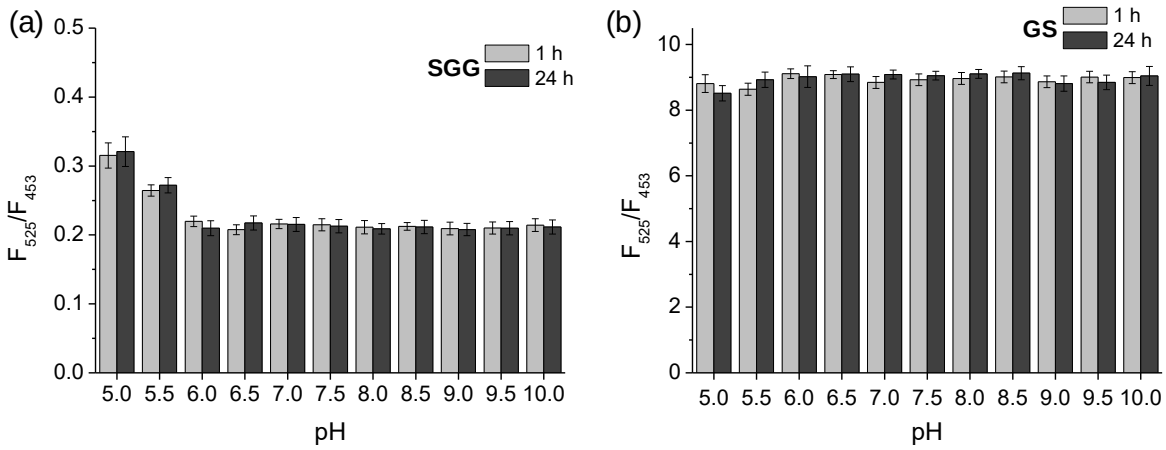

Figure S8. Effect of pH (range: 5 to 10) on the fluorescence ratios (F_{525}/F_{453}) for (a) **SGG** and (b) **GS** in universal buffer (100 mM citric acid, 100 mM KH_2PO_4, 100 mM $Na_2B_4O_7$, 100 mM Tris, 100 mM KCl) at 37 °C. The excitation wavelength was 363 nm (n = 10).

Cell Culture. All the cells were plated on glass-bottom dishes (Wuxi NEST Biotechnology) for 2 days before imaging and kept in a CO_2 incubator (Water Jacketed 3010, Thermo Fisher Scientific) under a humidified atmosphere of 5/95 (v/v) of CO_2/air at 37 °C. For labeling, the growth media was removed and replaced with glucose-free media. The cells were incubated with 5 μM **SGG** or **GS** for an additional 30 min, washed twice with PBS (Gibco, Thermo Fisher Scientific), and then imaged. The growth media for each cell are as follows.

HT-29 (human colorectal adenocarcinoma cell line, HTB-38, American Type Culture Collection): RPMI (WelGene, Korea) supplemented with 10% FBS (WelGene, Korea), penicillin (100 units/ml), and streptomycin (100 μg/mL).

HCT 116 (human colorectal carcinoma cell line, CCL-247, American Type Culture Collection), RKO (human colon carcinoma cell line, CRL-2577, American Type Culture Collection), SW-837 (human rectum adenocarcinoma cell line, CCL-235, American Type Culture Collection), and CCD-18Co (human colon normal cell line, CRL-1459, American Type Culture Collection): DMEM (WelGene, Korea) supplemented with 10% FBS (WelGene, Korea), penicillin (100 units/ml), and streptomycin (100 μg/mL).

HeLa (human cervical adenocarcinoma cell line, CCL-2, American Type Culture Collection): MEM (WelGene, Korea) supplemented with 10% FBS (WelGene, Korea), penicillin (100 units/ml), and streptomycin (100 μg/mL).

Cell Viability Test. To confirm whether **SGG** affects the viability of HT-29 and HCT 116 cells in live sample experiments, CCK-8 kit (Cell Counting kit-8, Dojindo) assays were conducted according to the protocol.

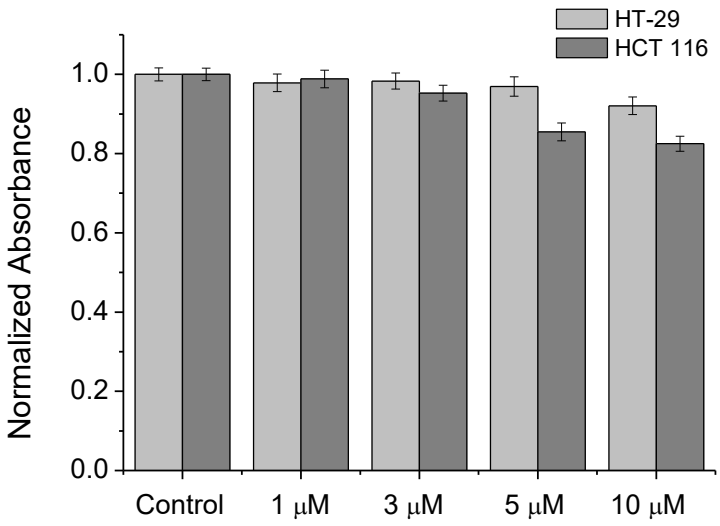

Figure S9. Viability test of HT-29 (light gray bars) and HCT 116 (dark gray bars) cells in the presence of **SGG** examined by using CCK-8 assay. The cells were incubated with **SGG** for 2 h (n = 6).

Two-Photon Microscopy. TPM imaging experiments were performed using a multiphoton microscope (TCS SP8 MP with DMI6000B, Leica Microsystems) by exciting **SGG** or **GS**-labeled cells and tissues with an ultrafast Ti:sapphire laser (Mai Tai HP, Spectra-Physics). The TP excitation wavelength was 740 nm with an average output power of 2478 mW, which corresponds to approximately 4.10×10^8 mW cm^{-2} at the focal plane. TPM fluorescence signals in the whole channel (400–600 nm) and ratio channels (Ch_{blue}: 400–450 nm, Ch_{green}: 500–600 nm) were obtained. Pseudocolored ratiometric data processing and analysis was performed using microscopy automation and image analysis software (MetaMorph NX, Molecular Devices). During the TPM experiments, the cell incubator system (Chamlide IC, Live Cell Instrument) was adapted to the multiphoton microscope for the stability of the live samples by maintaining suitable conditions (temperature, humidity, CO_2, and O_2) for long-term imaging.

Photostability Test. The photostability of **SGG** was determined by monitoring the changes in TPEF intensity with time of **SGG**-labeled (5 μM) HT-29 cells chosen without bias. The cells were incubated with 5 μM **SGG** for 30 min (sufficient β-gal reaction period), washed twice with PBS (Gibco, Thermo Fisher Scientific), and then imaged. The average TPEF intensities obtained at F_{blue} (400–450 nm) and F_{green} (500–600 nm) were constant for 1 h, indicating that **SGG** is highly photostable.

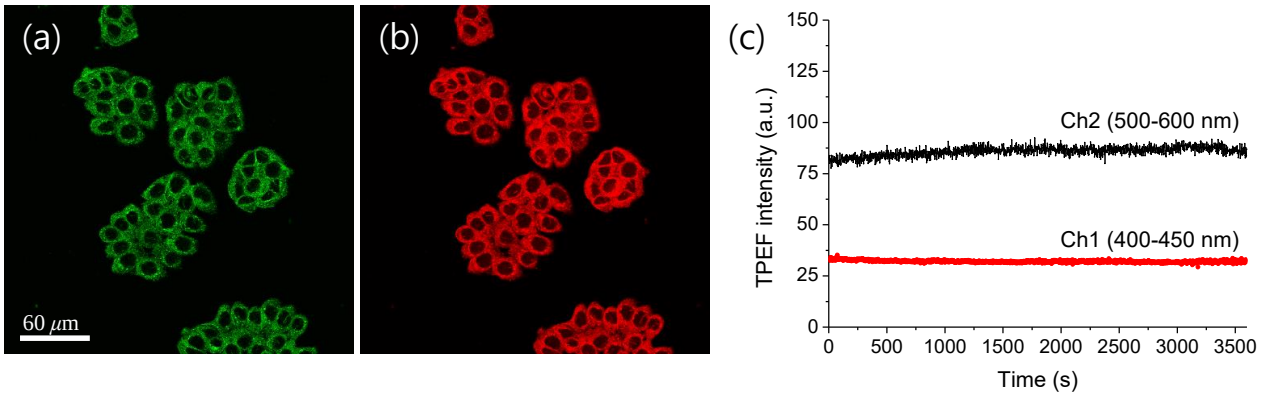

Figure S10. Photo-stability test of **SGG** (5 μM) in HT-29 cells. The cells were incubated with 5 μM **SGG** for 30 min (sufficient β-gal enzyme reaction period), washed twice with PBS and then imaged. The TPEF intensities collected at 400−450 nm (a, Ch1), and 500−600 nm (b, Ch2) with 740 nm excitation. (c) Plot of the average TPEF intensities inside the cells in each channel with 2 s intervals for 1 h (n = 3).

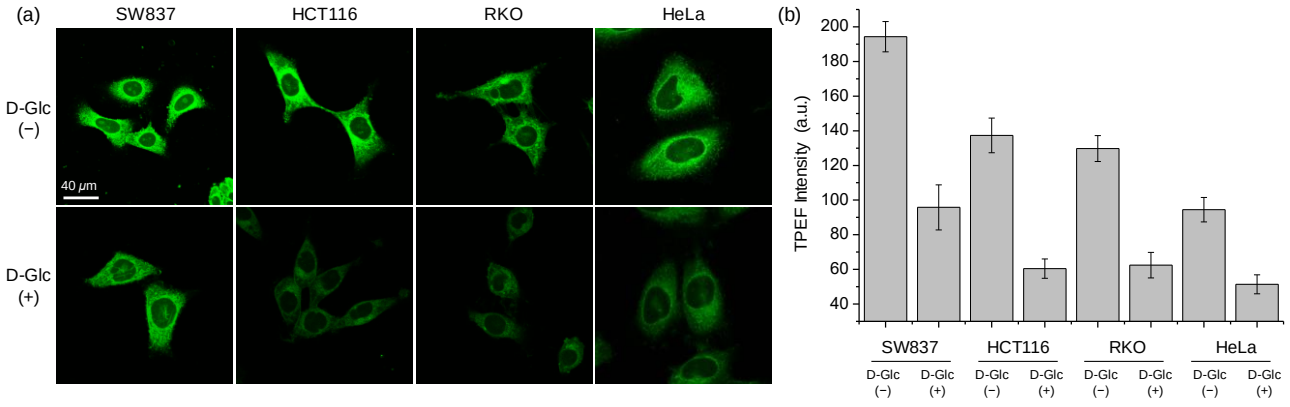

Figure S11. TPM images (a) and plot of the TPEF intensities (b) of **GS** in various cancer cell lines with or without 55 mM of D-glucose (n = 100).

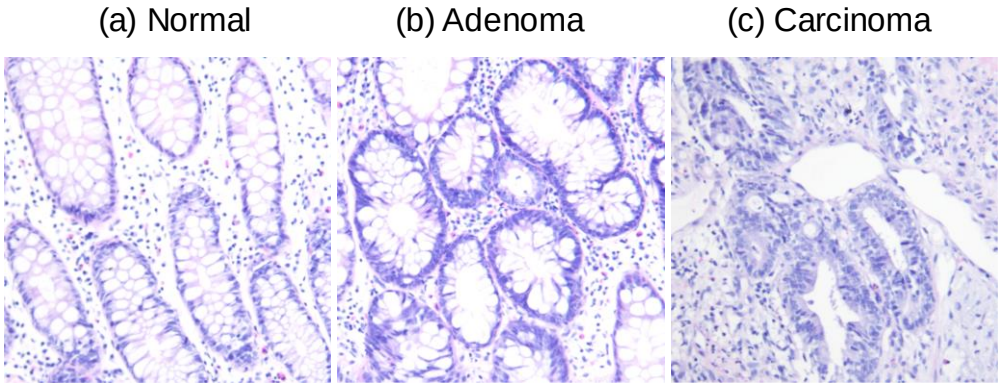

Figure S12. Pathologic findings by hematoxylin and eosin (H&E)-stain of normal mucosa (a), tubular adenoma (b) and carcinoma (c) in colon tissue with 200× magnification.

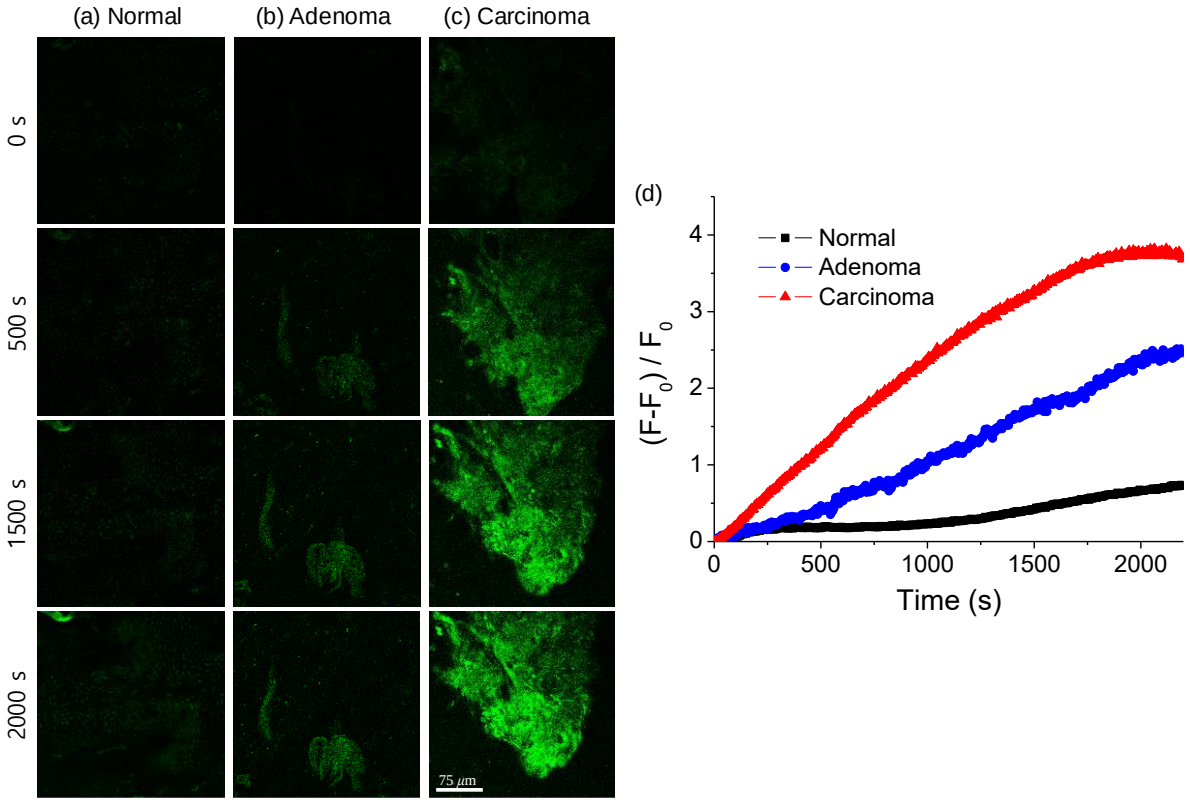

Figure S13. (a–c) TPM images of real time uptake of **SGG** (10 μM) in human colon (a) normal, (b) adenoma, and (c) carcinoma tissues. (d) Plot of the relative TPEF intensity of the probe inside the tissues with 5 s intervals (n = 5).

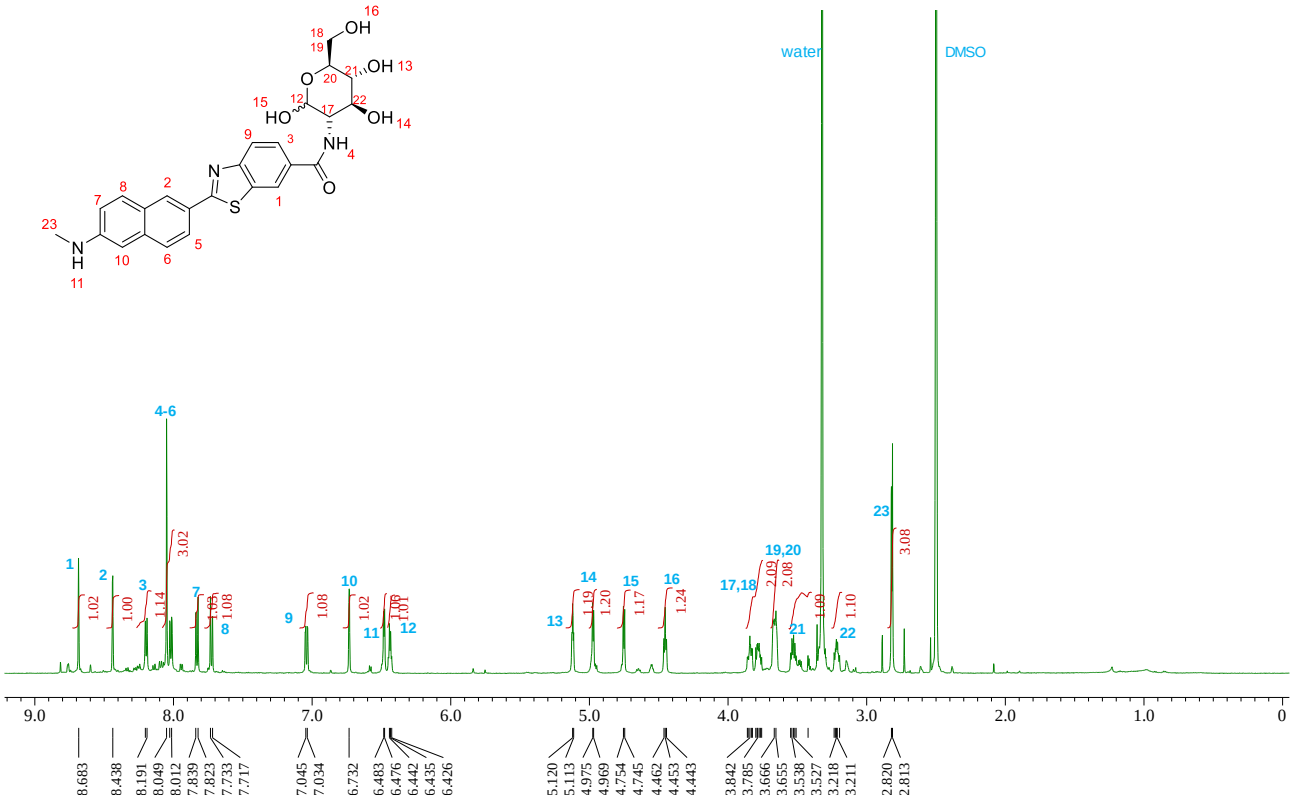

Figure S14. ^{1}H-NMR spectrum (600 MHz) of **GS** in DMSO-*d*$_6$.

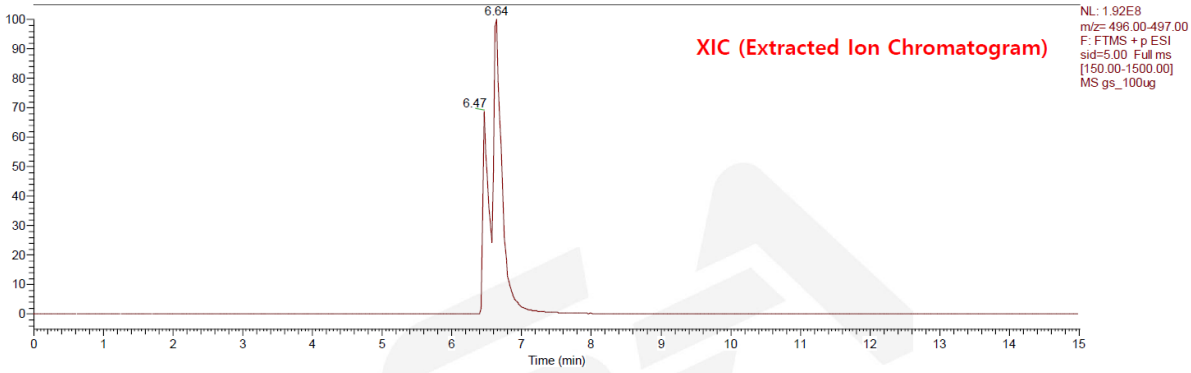

[5-1] MS Spectrum : RT 6.47

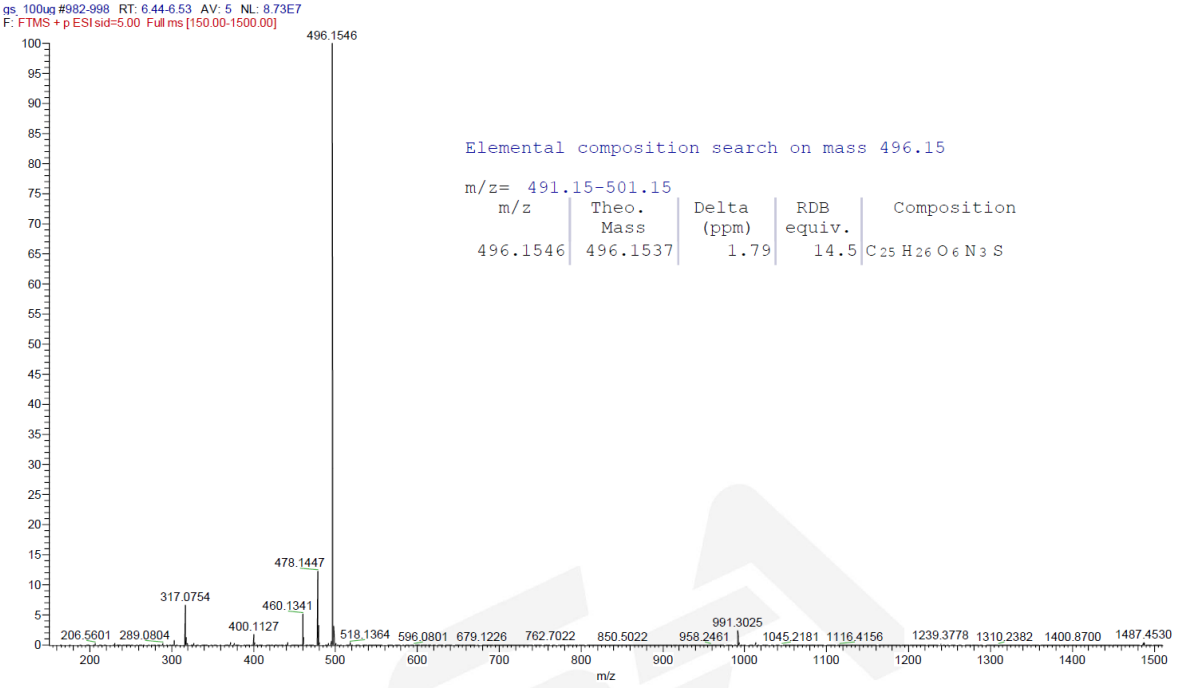

Elemental composition search on mass 496.15

m/z= 491.15-501.15

m/z	Theo. Mass	Delta (ppm)	RDB equiv.	Composition
496.1546	496.1537	1.79	14.5	$C_{25}H_{26}O_6N_3S$

[5-2] MS Spectrum : RT 6.64

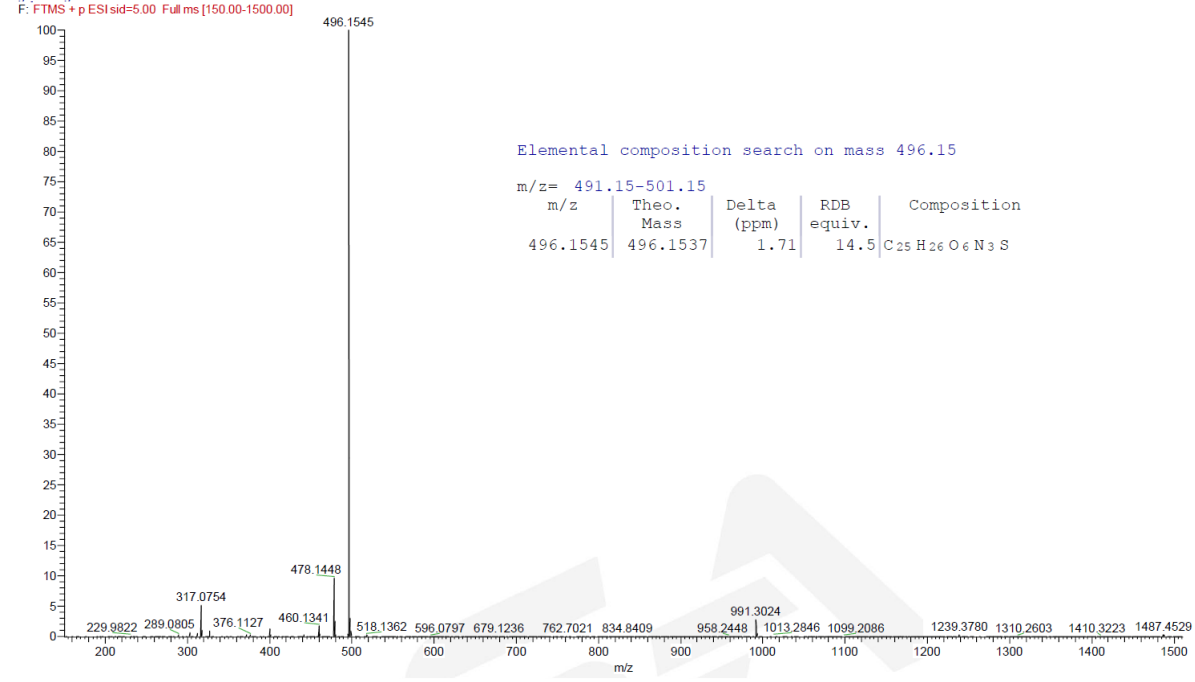

Elemental composition search on mass 496.15

m/z= 491.15-501.15

m/z	Theo. Mass	Delta (ppm)	RDB equiv.	Composition
496.1545	496.1537	1.71	14.5	$C_{25}H_{26}O_6N_3S$

Figure S15. HRMS analysis of **GS.** α and β anomers of **GS** showed same mass (m/z = 496.1545).

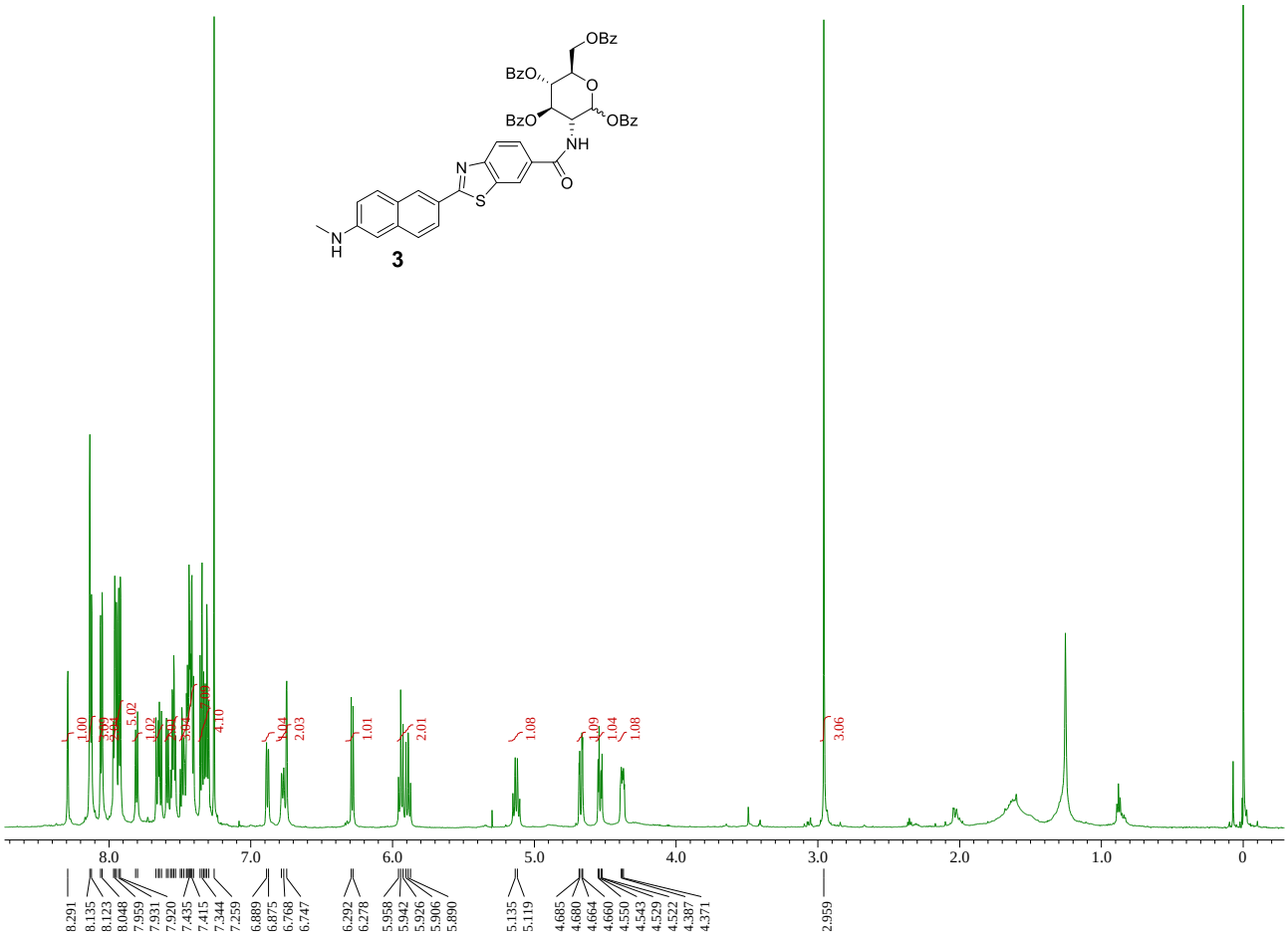

Figure S16. ^{1}H-NMR spectrum (600 MHz) of **3** in $CDCl_3$.

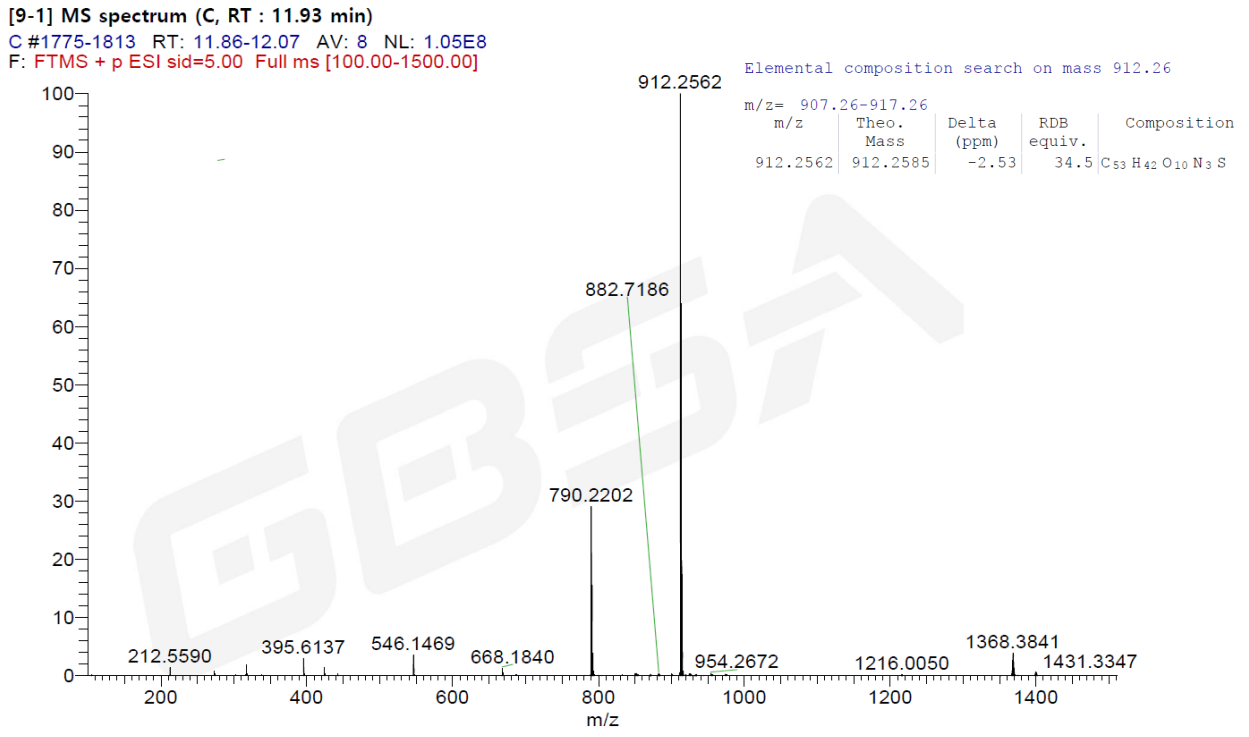

Figure S17. HRMS analysis of **3**.

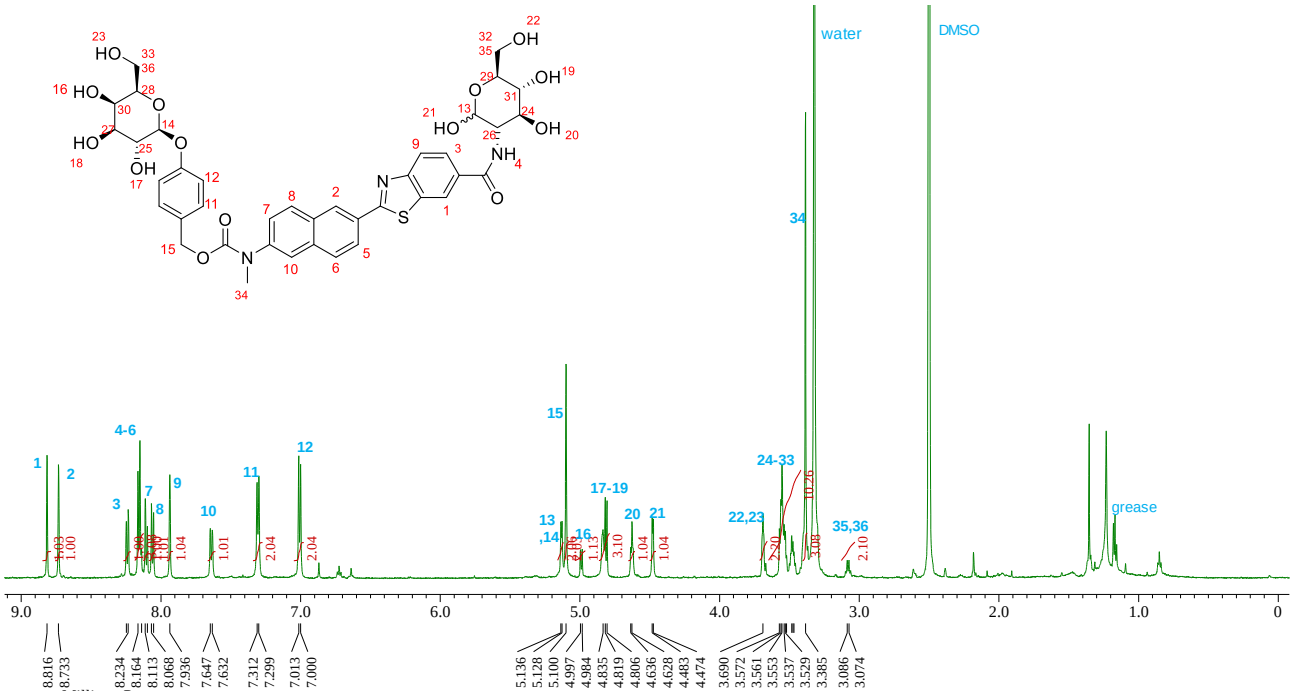

Figure S18. ^{1}H-NMR spectrum (600 MHz) of **SGG** in DMSO-d_6.

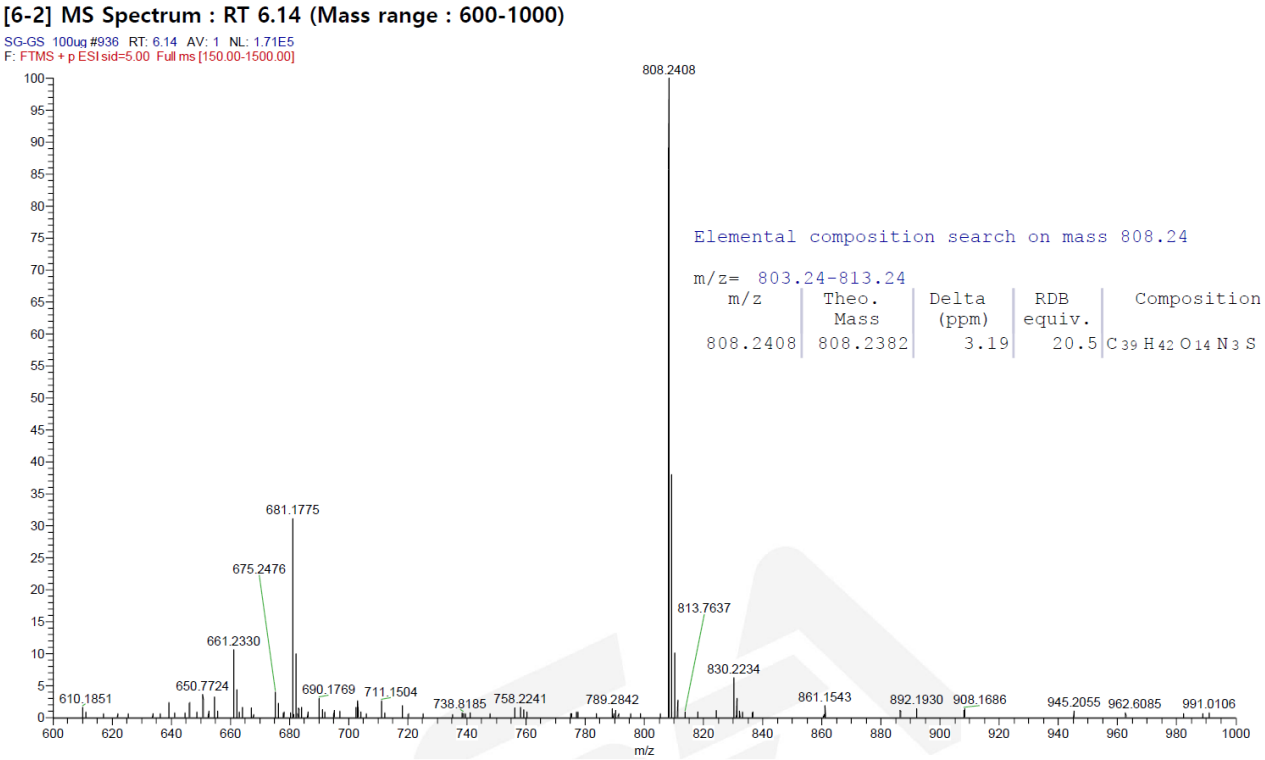

Figure S19. HRMS analysis of **SGG**.

References

1 Lim, C. S.; Masanta, G.; Kim, H. J.; Han, J. H.; Kim, H. M.; Cho, B. R., Ratiometric detection of mitochondrial thiols with a two-photon fluorescent probe. *J. Am. Chem. Soc.* **2011**, *133*, 11132–11135.

2 Carmona, J. A.; Gonzalo, G.; Serrano, I.; Crespo-Pena, A. M.; Simek, M.; Monge, D.; Fernandez, R.; Lassaletta, J. M., Asymmetric organocatalytic synthesis of tertiary azomethyl alcohols: key intermediates towards azoxy compounds and alpha-hydroxy-beta-amino esters. *Org. Biomol. Chem.* **2017**, *15*, 2993–3005.

3 Lee, H. W.; Heo, C. H.; Sen, D.; Byun, H. O.; Kwak, I. H.; Yoon, G.; Kim, H. M., Ratiometric two-photon fluorescent probe for quantitative detection of beta-galactosidase activity in senescent cells. *Anal. Chem.* **2014**, *86*, 10001–10005.

4 Brouwer, A. M., Standards for photoluminescence quantum yield measurements in solution (IUPAC Technical Report). *Pure Appl. Chem.* **2011**, *83*, 2213–2228.

5 Kim, H. M.; Choo, H. J.; Jung, S. Y.; Ko, Y. G.; Park, W. H.; Jeon, S. J.; Kim, C. H.; Joo, T.; Cho, B. R., A two-photon fluorescent probe for lipid raft imaging: C-laurdan. *Chembiochem* **2007**, *8*, 553–559.

6 Lee, S. K.; Yang, W. J.; Choi, J. J.; Kim, C. H.; Jeon, S. J.; Cho, B. R., 2,6-Bis[4-(p-dihexylaminostyryl)styryl]anthracene derivatives with large two-photon cross sections. *Org. Lett.* **2005**, *7*, 323–326.

7 Makarov, N. S.; Drobizhev, M.; Rebane, A., Two-photon absorption standards in the 550–1600 nm excitation wavelength range. *Opt. Express* **2008**, *16*, 4029–4047.